

# Production of charged hadrons with large transverse momenta in $pp$ collisions at 70 GeV

V. V. Abramov, A. V. Alekseev, B. Yu. Baldin, S. I. Bitjukov, Yu. N. Vrazhnov, V. Yu. Glebov, A. S. Dyshkant, V. N. Evdokimov, V. V. Zmushko, A. N. Krinitsyn, V. I. Kryshkin, N. Yu. Kul'man, Yu. M. Mel'nik, R. M. Sulyaev, and L. K. Turchanovich

*Joint Institute for Nuclear Research*

(Submitted 27 January 1981)

Pis'ma Zh. Eksp. Teor. Fiz. **33**, No. 5, 304–309 (5 March 1981)

The invariant cross sections for production of  $\pi^\pm$ ,  $K^\pm$ ,  $p$ , and  $\bar{p}$  and the ratios of particle yields in the transverse momentum range of 1.0 to 4.1 GeV/c at 90° angle in the c.m.s. were measured. The dependences of the cross sections and of the meson-yield ratios on energy and on  $X_1 = 2P_\perp/\sqrt{s}$  are described qualitatively by the model based on quantum chromodynamics.

PACS numbers: 13.75.Cs

The measurements were performed with use of a focusing, double-arm spectrometer (FDS) with drift tubes and threshold Cerenkov counters.<sup>1</sup> The experiment involved the use of a proton beam with an intensity up to  $10^{12}$  protons per cycle, which was slowly extracted from the accelerator. This experiment is a continuation of our first experiment in which the beam had an intensity up to  $10^8$  protons per cycle.<sup>1</sup>

The invariant cross sections for production of  $\pi^\pm$ ,  $K^\pm$ ,  $p$ , and  $\bar{p}$  in  $pp$  collisions are given as a function of  $P_\perp$  in Table I. The errors include the statistical errors of the experimental data and of the spectrometer-acceptance Monte Carlo calculations. The estimated accuracy of the absolute value of the cross sections is 15%. The cross section for  $\bar{p}$  has the maximum rate of decrease with increasing  $P_\perp$  and the correction for  $p$  has minimum rate of decrease.

As shown by us in Ref. 1, a strong scaling violation occurs in the region of transverse momenta  $< 2.2$  GeV/c at 70 GeV

$$E \frac{d^3\sigma}{d^3p} = g(P_\perp) f(X_1), \quad (1)$$

where  $X_1 = 2P_\perp/\sqrt{s}$  and  $\sqrt{s}$  is the total energy of colliding protons in the c.m.s. Such scaling, which was predicted by the component-exchange model,<sup>2</sup> can be approximately achieved experimentally at energies  $> 200$  GeV (see Fig. 1). Figure 1 shows the dependence on  $X_1$  of the invariant cross section for production of  $\pi^-$  mesons  $E d^3\sigma/d^3p$ , which is divided by  $g(P_\perp) = (P_\perp^2 + 0.66)^{-4.03}$ . A  $g(P_\perp)$  function of this type was obtained as a result of approximation of the experimental data in the region  $0.5 \leq P_\perp \leq 7$  GeV/c and  $E \geq 200$  GeV.<sup>3,4</sup> This function for mesons behaves in a well-known manner  $g(P_\perp) = P_\perp^{-8}$  at large  $P_\perp$ .

The experimental data lie well above the scaling dependence at 70 GeV. The diver-

TABLE I.

$P_L$ GeV/c	$\pi^+$	$\pi^-$	$K^+$	$K^-$	$p$	$\bar{p}$
1,748	$(3,79 \pm 0,09) \cdot 10^{-3}$	$(2,60 \pm 0,07) \cdot 10^{-3}$	$(1,09 \pm 0,04) \cdot 10^{-3}$	$(3,51 \pm 0,21) \cdot 10^{-4}$	$(3,78 \pm 0,09) \cdot 10^{-3}$	$(1,13 \pm 0,07) \cdot 10^{-4}$
1,993	$(1,02 \pm 0,03) \cdot 10^{-3}$	$(6,60 \pm 0,18) \cdot 10^{-4}$	$(3,13 \pm 0,10) \cdot 10^{-4}$	$(8,87 \pm 0,37) \cdot 10^{-5}$	$(1,19 \pm 0,03) \cdot 10^{-3}$	$(2,53 \pm 0,13) \cdot 10^{-5}$
2,561	$(4,84 \pm 0,15) \cdot 10^{-5}$	$(2,91 \pm 0,08) \cdot 10^{-5}$	$(1,71 \pm 0,06) \cdot 10^{-5}$	$(3,91 \pm 0,26) \cdot 10^{-6}$	$(7,38 \pm 0,21) \cdot 10^{-5}$	$(8,28 \pm 0,76) \cdot 10^{-7}$
2,889	$(8,38 \pm 0,26) \cdot 10^{-6}$	$(4,48 \pm 0,12) \cdot 10^{-6}$	$(3,01 \pm 0,11) \cdot 10^{-6}$	$(5,66 \pm 0,23) \cdot 10^{-7}$	$(1,42 \pm 0,04) \cdot 10^{-5}$	$(1,05 \pm 0,09) \cdot 10^{-7}$
3,256	$(1,02 \pm 0,03) \cdot 10^{-6}$	$(5,43 \pm 0,17) \cdot 10^{-7}$	$(3,76 \pm 0,17) \cdot 10^{-7}$	$(5,98 \pm 0,36) \cdot 10^{-8}$	$(2,04 \pm 0,06) \cdot 10^{-6}$	$(6,94 \pm 0,02) \cdot 10^{-9}$
3,655	$(1,04 \pm 0,04) \cdot 10^{-7}$	$(5,04 \pm 0,24) \cdot 10^{-8}$	$(3,95 \pm 0,21) \cdot 10^{-8}$	$(5,32 \pm 0,57) \cdot 10^{-9}$	$(2,69 \pm 0,08) \cdot 10^{-7}$	$(1,02 \pm 0,29) \cdot 10^{-9}$
2,885	$(2,51 \pm 0,12) \cdot 10^{-8}$	$(1,02 \pm 0,06) \cdot 10^{-8}$	$(0,43 \pm 0,83) \cdot 10^{-9}$	$(1,02 \pm 0,19) \cdot 10^{-9}$	$(7,21 \pm 0,29) \cdot 10^{-8}$	—
4,100	$(5,45 \pm 0,31) \cdot 10^{-9}$	$(1,78 \pm 0,18) \cdot 10^{-9}$	$(2,25 \pm 0,18) \cdot 10^{-9}$	$(2,04 \pm 0,55) \cdot 10^{-10}$	$(1,79 \pm 0,06) \cdot 10^{-8}$	—

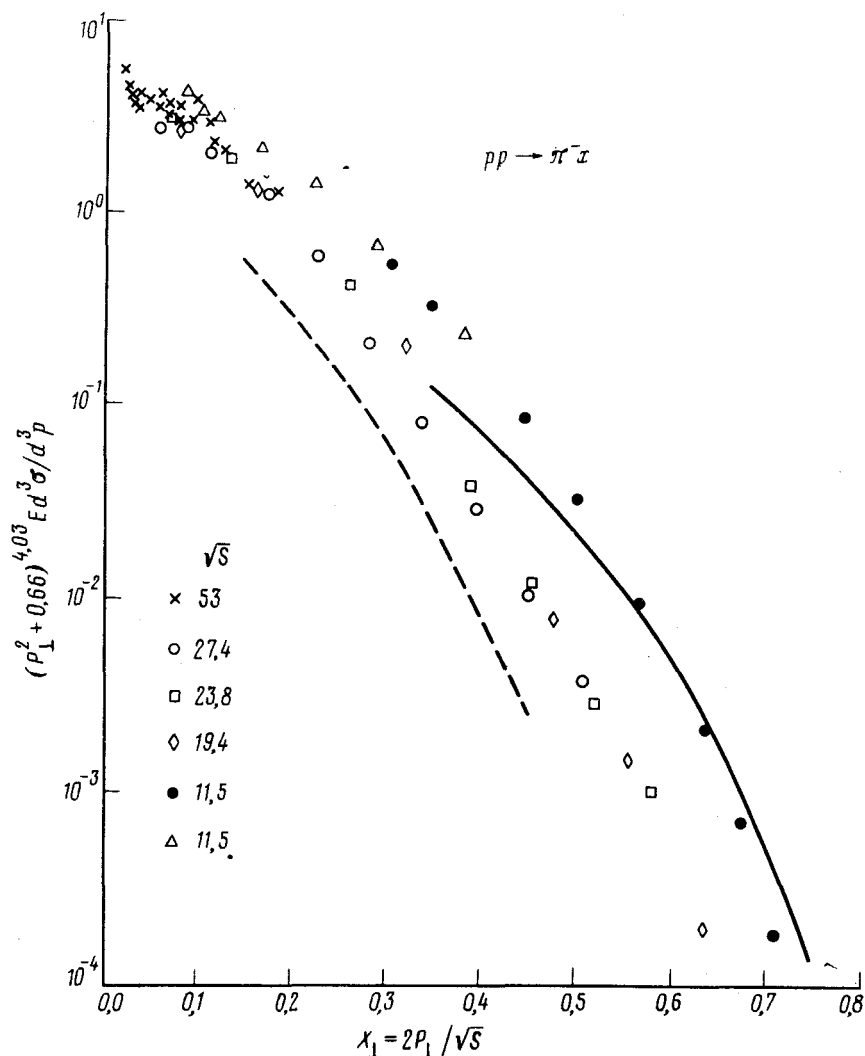


Fig. 1. Invariant cross section for production of  $\pi^-$  mesons ( $mb/\text{GeV}^2$ ) multiplied by  $(P_\perp^2 + 0.66)^{4.03}$  as a function of  $X_\perp$ .  $\bullet$  represent the results of our investigation;  $\Delta$  represent the data of Ref. 1;  $\times$  denote the data of Ref. 3;  $\circ$  and  $\square$ , data of Ref. 4. The solid curve represents a QCD calculation for  $\sqrt{s} = 11.5$  GeV and the dashed curve denotes a QCD calculation for  $\sqrt{s} = 27.4$  GeV.

gence increases with  $P_\perp$  and reaches a value of about 10 at  $X_\perp = 0.63$ . Figure 1 also shows the results of a calculation of two energies according to the model based on quantum chromodynamics (QCD), which is analogous to that in Ref. 5. We can see that the dependence of the invariant cross sections on  $P_\perp$  or  $X_\perp$  and the magnitude of the scaling violation (1) are correctly predicted by this model. The difference between the absolute values of calculations and the experimental data (2–3 fold) corresponds to the magnitude of the uncertainty of the model. The component-exchange model, which predicts the scaling (1) with  $g(P_\perp) = P_\perp^{-8}$ , describes the data

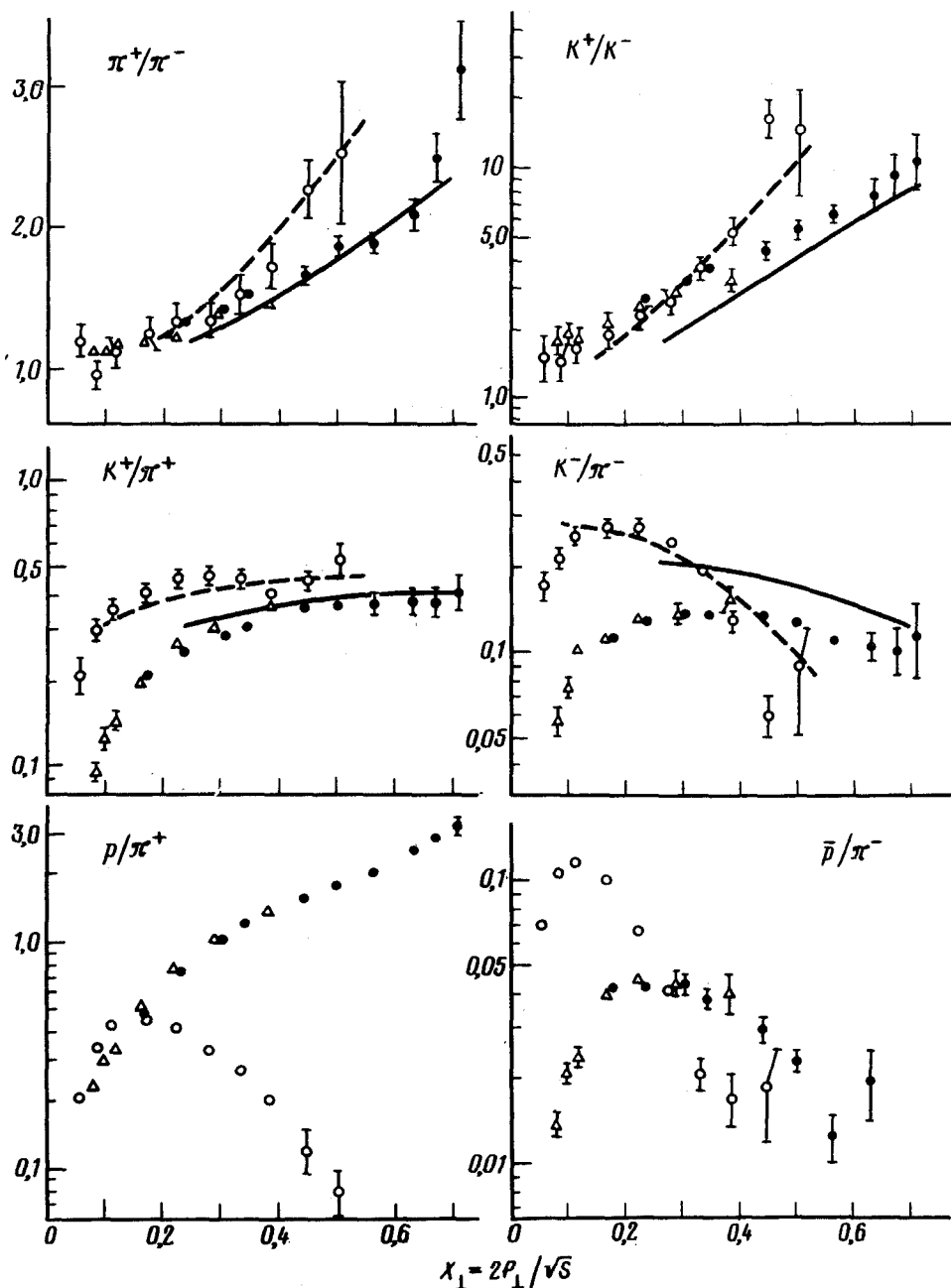


Fig. 2. Ratio of the particle yields as a function of  $X$ .  $\bullet$ , results of our investigation, 70 GeV;  $\blacktriangle$ , data of Ref. 1, 70 GeV;  $\circ$ , data of Ref. 4, 400 GeV. The solid curve represents a QCD calculation for 70 GeV and the dashed curve denotes a QCD calculation for 400 GeV.

poorly for 70 GeV.

The particle-yield ratios are shown in Fig. 2, which also shows, for comparison, the data for 400 GeV (Fig. 4), those of our preceding experiment,<sup>1</sup> and the results of calculations based on QCD for 70 GeV and 400 GeV.

We can see in Fig. 2 that the ratios  $\pi^+/\pi^-$  and  $K^+/K^-$  for 70 GeV are systematically lower than those for 400 GeV. An analysis of the calculations shows that this variation of the ratios with the energy for a specified  $X_1$  is associated primarily with the quantum chromodynamic  $Q^2$  dependence of the distribution and fragmentation functions.

The dependence of the particle-yield ratios on  $X_1$  is the same for 400 GeV and for 70 GeV, except for the  $p/\pi^+$  ratio.

The QCD calculations describe the dependence of the ratios  $\pi^+/\pi^-$ ,  $K^+/K^-$ ,  $K^+/\pi^+$  and  $K^-/\pi^-$  on  $X_1$  and on the energy qualitatively correctly. The best quantitative agreement is obtained for the ratios  $\pi^+/\pi^-$  and  $K^+/\pi^+$ , which contain the valence quarks of colliding protons. The ratios  $K^+/K^-$  and  $K^-/\pi^-$  are predicted more poorly by the model, which seems to indicate that the cross section for production of  $K^-$  mesons, in which the valence quarks of colliding protons are missing, is currently difficult to calculate. The production of  $p$  and  $\bar{p}$  baryons, in contrast with the production of mesons, is not described by the QCD model.

1. V. V. Abramov *et al.*, *Yad. Fiz.* **31**, 1483 (1980) [*Sov. J. Nucl. Phys.* **31**, (1980)].
2. B. Blankenbecler *et al.*, *Phys. Rev.* **D12**, 3469 (1975).
3. B. Alper *et al.*, *Nucl. Phys.* **B100**, 237 (1975).
4. D. Antreasyan *et al.*, *Phys. Rev.* **D19**, 764 (1979).
5. R. P. Feynman, R. D. Field, and G. Fox, *Phys. Rev.* **D18**, 3320 (1978).

Translated by S. J. Amoretti

Edited by Robert T. Beyer